(NASA-CR-121259) HIGH TEMPERATURE, LOW-CYCLE FATIGUE OF COPPER-BASE ALLOYS IN ARGON PART 1: PRELIMINARY RESULTS FOR 12 (Mar-Test, Inc , Cincinnati, Ohio) ~~52~~ 51 p HC $4 75 CSCL 11F G3/17

N74-14190

Unclas 26072

NASA CR-121259

HIGH TEMPERATURE, LOW-CYCLE FATIGUE OF COPPER-BASE ALLOYS IN ARGON; PART I - PRELIMINARY RESULTS FOR 12 ALLOYS AT 1000° F (538° C)

by: J.B.Conway, R.H.Stentz and J.T.Berling

MAR-TEST INC.

Cincinnati, Ohio

January 1973

prepared for

NATIONAL AERONAUTICS AND SPACE ADMINISTRATION

NASA Lewis Research Center
Contract NAS3-16753

G.R.Halford, Project Manager

1. Report No.	2. Government Accession No.	3. Recipient's Catalog No.
NASA CR-121259		

4. Title and Subtitle	5. Report Date
High Temperature, Low-Cycle Fatigue of Copper-Base Alloys in Argon; Part I - Preliminary Results for 12 Alloys at 1000° F (538° C)	January 1973
	6. Performing Organization Code
7. Author(s)	8. Performing Organization Report No.
J. B. Conway, R. H. Stentz and J. T. Berling	
	10. Work Unit No.
9. Performing Organization Name and Address Mar-Test Inc. 45 Novner Drive Cincinnati, Ohio, 45215	11. Contract or Grant No. NAS 3-16753
	13. Type of Report and Period Covered Contractor Report
12. Sponsoring Agency Name and Address National Aeronautics and Space Administration Lewis Research Center 21000 Brookpark Rd., Cleveland, Ohio 44135	14. Sponsoring Agency Code

15. Supplementary Notes

Project Manager, Dr. G. Halford, NASA-Lewis Research Center, Cleveland, Ohio

16. Abstract

This is a data summary report on Task 1 of Contract NAS3-16753, High Temperature, Low-Cycle Fatigue of Copper-Base Alloys. It involves short-term tensile evaluations at room temperature and 538°C and low-cycle fatigue evaluations at 538°C for the following materials:

- Zirconium copper-annealed
- Zirconium copper-1/4 hard
- Zirconium copper-1/2 hard
- Tellurium copper-1/2 hard
- Chromium copper-SA and aged
- OFHC copper-hard
- OFHC copper-1/4 hard
- OFHC copper-annealed
- Silver-as drawn
- Zr-Cr-Mg copper-SA, CW and aged
- Electroformed copper-30-35 ksi
- Co-Be-Zr- copper-SA and aged

A total of 50 tensile tests and 76 low-cycle fatigue tests were performed using a strain rate of 0.2 percent per second.

17. Key Words (Suggested by Author(s))	18. Distribution Statement
	Unclassified - Unlimited

19. Security Classif. (of this report)	20. Security Classif. (of this page)	21. No. of Pages	22. Price*
Unclassified	Unclassified		

* For sale by the National Technical Information Service, Springfield, Virginia 22151

NASA-C-168 (Rev. 6-71)

INTRODUCTION

In the past, regeneratively cooled rocket engine thrust chambers have been required to sustain one,or in some instances only several, hot operating cycles. However, the current requirements of reusability for standard cycle applications such as the Space Shuttle or the Space Tug engines have introduced the problem of low cycle thermal fatigue. High performance operating conditions produce a severe thermal environment. To withstand these thermal conditions as well as the cyclic operation, the thrust chamber materials must have high thermal conductivity and high thermal fatigue resistance.

Copper-base alloys have these qualities. However, sufficient thermal fatigue data did not exist prior to the program to allow a selection of the most capable material. There had been some fatigue studies made of several selected copper-base alloys. These studies were done by several sources. Variations in data due to the variations in test samples and test procedures produced inconclusive results. Also, early low cycle thermal fatigue failures of actual thrust chambers produced more questions than answers.

This overall test program is being conducted to provide data under repeatable controlled conditions that could be used to compare all likely candidate materials, provide a basis for thrust chamber design and information for low cycle thermal fatigue prediction methods. Eleven copper base alloys and silver were tested to provide strength and isothermal fatigue data. This initial screening would yield one or more materials that would then be more fully characterized. The detailed study of low cycle fatigue behavior of the material or materials selected will be performed in the second task and will be reported separately.

After the characterizations are completed, actual thrust chamber test hardware will be made from the best materials and tested for its cyclic life. All of the information obtained for these materials would be used in conjunction with analytical thermal cyclic life predictions for designing thrust chambers for long time reusability requirements.

I - TEST EQUIPMENT

A closed-loop, servo-controlled, hydraulically-actuated fatigue machine (see Figure 1) was employed in this program. This machine was equipped with the necessary recorders to provide continuous readouts of the desired test information.

A block diagram of the type of test machine used is presented in Figure 2. The programmer is a precision solid-state device capable of furnishing all of the required waveform signals necessary to provide the strain or stress values demanded in the test. This signal is compared in the summing network with the strain or stress values actually present at the specimen at any instant of time. Any deviation from the required parameter is sensed by the servo-controller which supplies a correction current signal to the servo-valve which provides the correct hydraulic flow and pressure to the hydraulic actuator. The actuator in turn imparts the necessary displacement and force through the load cell to the specimen. The diametral displacement of the specimen in the gage section is sensed by the extensometer and the motion is imparted to the LVDT (Linear variable displacement transducer) which supplies an electrical signal to the analog computer. The analog computer accepts the instantaneous diametral strain and axial force signals and operates upon them to provide signals representing all of the

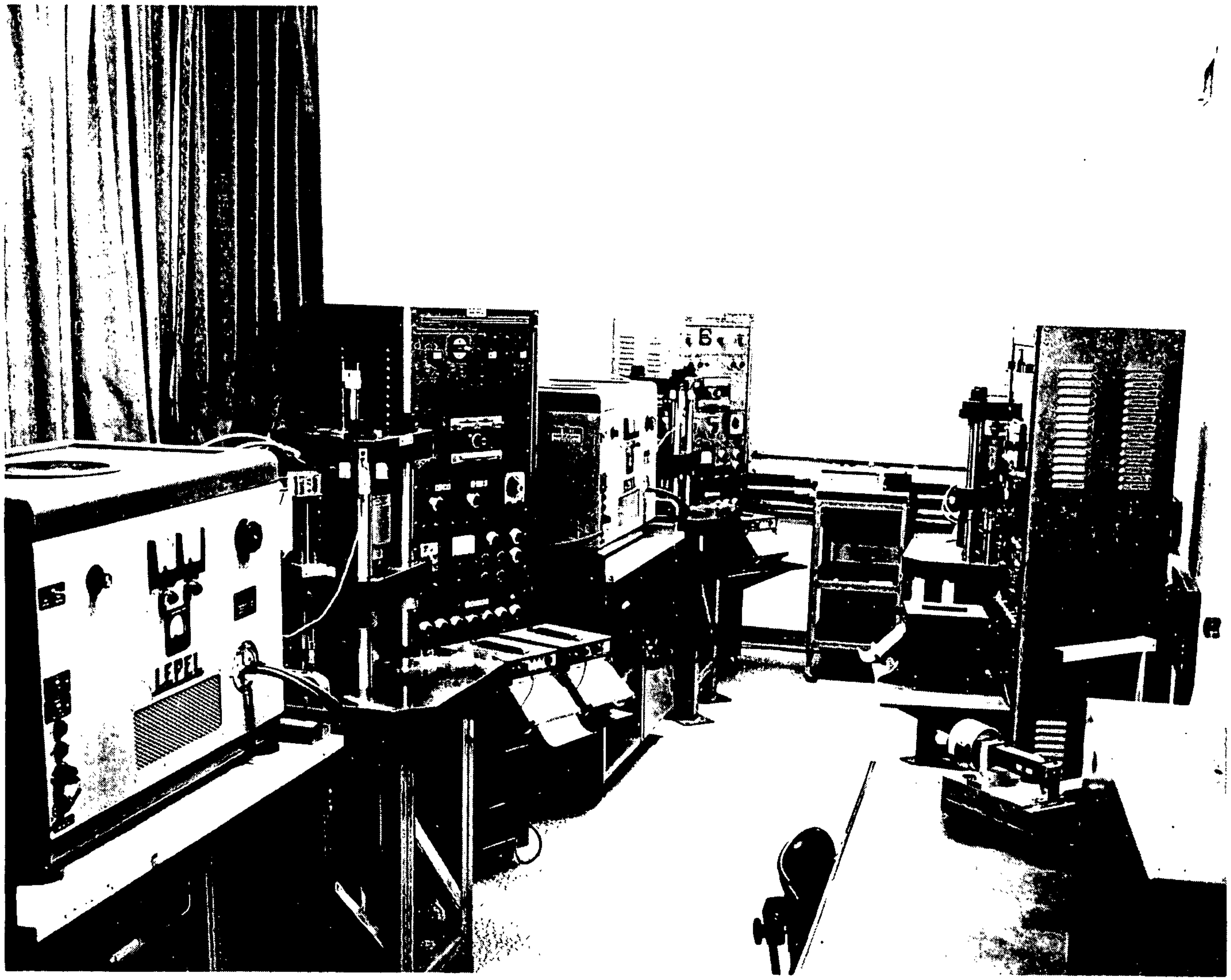

Figure 1. - Fatigue laboratory at Mar-Test Inc. showing three high temperature fatigue machines.

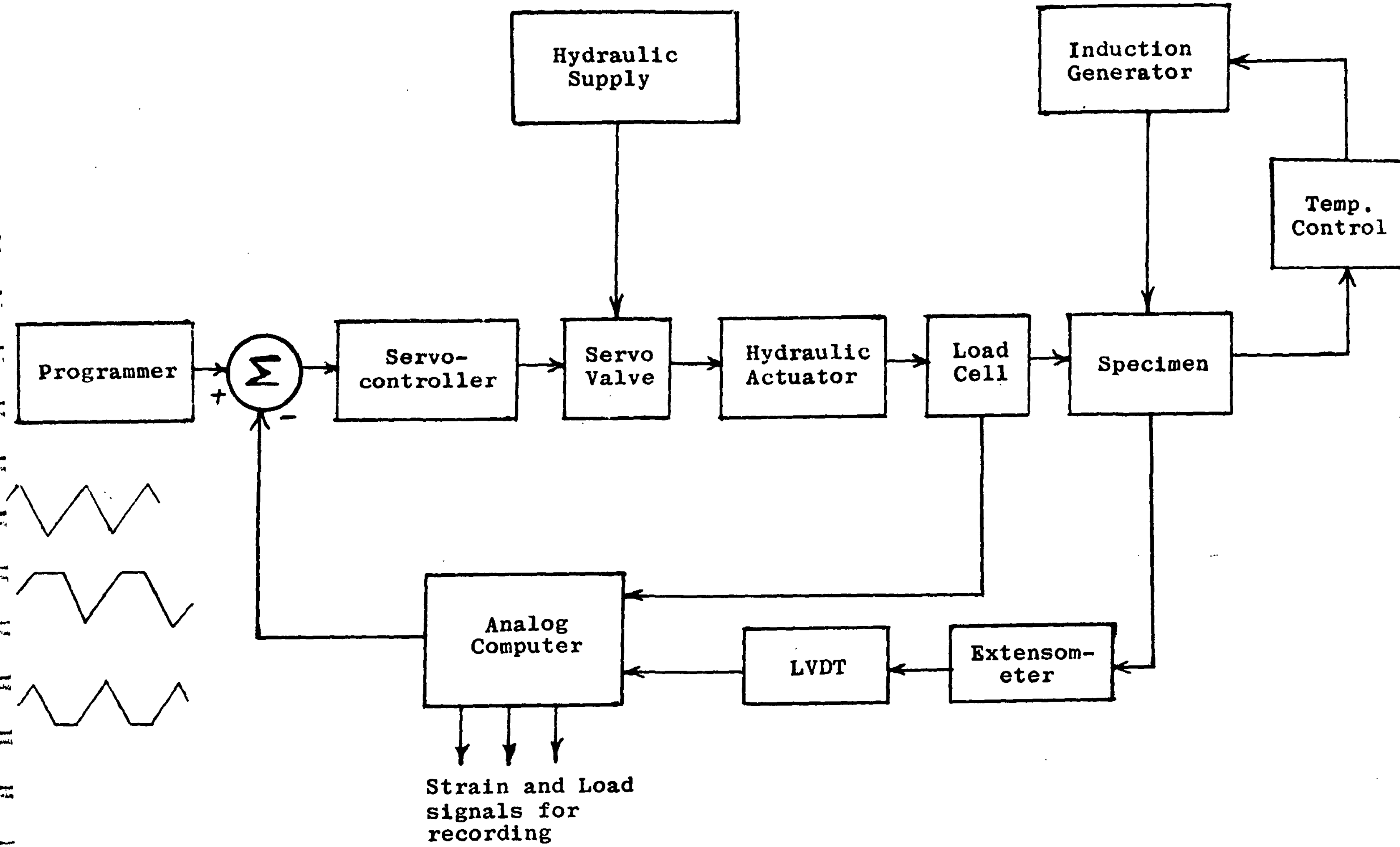

Figure 2- Schematic of components in fatigue testing machine.

strain and stress components of interest. Any one of these can be selected for comparison with the programmer signal.

Manufacturer and nomenclature of the various components of the fatigue machines are as follows:

1. Programmer - designed and built by Mar-Test Inc.
2. Servo-controller - designed and built by Mar-Test Inc.
3. Actuator - Universal Fluid Dynamics, Type MDF5-H-BR
4. Servo-valve - Moog, Model 76-101
5. Hydraulic System - Racine, Model PSV-SSO-20GRS
6. Load Cell - Strainsert, Model FFL15U-2SP(K)
7. Induction Generator - Lepel, Model T-2.5-1-KC-J-BW
8. Extensometer - designed and built by Mar-Test Inc. to measure diametral strain
9. LVDT - ATC, Model 6234A05B01XX
10. Analog Strain Computer - designed and built by Mar-Test Inc.
11. Load Frame and Fixtures - designed and built by Mar-Test Inc.

Each fatigue machine consists of a sturdy three-column support system connecting two fixed, horizontal platens. A movable platen operates between the fixed platens and is hydraulically actuated to provide the desired cyclic motion. The movable platen contains three close-tolerance bushings which slide on the chrome-plated support columns to impart extreme rigidity and precise alignment to the system.

The diametral strain at the minimum diameter point of the specimen is measured using a specially constructed diametral extensometer.This device was fabricated from low thermal expansion materials(quartz and invar) to minimize the effects of room temperature changes on extensometer output. Each extensometer is calibrated prior to use by employing a special calibration fixture. Each device is supported horizontally (that is, in the actual use position) with the extensometer knife edges touching a 0.25 inch diameter split pin. One of the pin halves is fixed and the other is displaced horizontally to simulate a diameter increase. This motion is controlled by the rotation of the barrel of a special micrometer(calibrated against NBS standard). In this way the extensometer is calibrated to within 10 microinches. With this type of calibration and a knowledge of the stability and accuracy of the electronic components of the system a reasonable estimate of the accuracy of the strain control system is 60 microinches per inch in terms of axial strain range.

Before any tests are made each load cell is calibrated in position by placing a calibrated(NBS) Ring-Force Gauge (Morehouse Instrument Co.,Model 5BT,5000 lbs capacity with an accuracy to 0.2 percent) in the specimen position in the load train. As the actuator is caused to apply a load the output of the load cell is plotted against the load indicated by the calibrated Ring-Force Gauge. This calibration is performed at frequent intervals to insure accurate stress measurements during the testing program.

Each fatigue machine has its own control console which functions to supply the very precise control features which are so essential to the performance of meaningful fatigue tests. In addition to housing the temperature controller and an elapsed time indicator each control console contains:

a) a calibration panel which also provides means for automatic or manual control of the hydraulic solenoid and power for auxiliary equipment such as the induction generator and recorders;

b) a programmer which provides the required demand signal waveform for the test;

c) an analog strain computer which generates the load and strain components for recording and control purposes;

d) a servo-controller which compares the programmer supplied demand signal and the computer supplied feedback signal and generates the proper control current for the servo-valve; a meter relay circuit operates in conjunction with the servo-controller to provide the means for shutting down the system when the specimen fails.

One of the important precautionary features of the Mar-Test fatigue machines is the incorporation of a manually operated by-pass valve across the hydraulic actuator. With this valve open the test specimen can not be exposed to any inadvertent load transients during start-up. The hydraulic solenoid valve can be energized with this valve open and the load transients frequently encountered in test start-up can be eliminated. Once the solenoid valve is opened the by-pass valve can be closed slowly to bring the system under control.During this operation the load trace is monitored so that a smooth transfer is effected and all load transients are eliminated.

II - SPECIMEN STORAGE AND PRE-TEST CLEANING

After being machined all specimens were wrapped in soft tissue paper and placed in individual hard plastic cylinders (about 3.5 inches in length and 7/8 inch inside diameter). The ends of these cylinders were then sealed with masking tape and the specimen code number was written on the external surface of the cylinder. These cylinders were used for storage before and after test.

In preparing for a test each specimen was subjected to the following:

1) a small longitudinal notch was filed in the threaded sections of the specimen; this was designed to aid in in the removal of entrapped air from the threaded area after the specimen was inserted in the adaptors (see below for specimen-adaptor assembly);
2) the specimen was washed with Freon to remove any surface oils which might have remained after machining;
3) a small quantity of dilute phosphoric acid was applied by hand to the complete surface of the specimen; this removed any surface oxides and any machining oil not removed by the cleaning with Freon; this operation was completed within 15 seconds;
4) the specimen was rinsed in warm water and dried using soft absorbent tissue;
5) the specimen was then subjected to a final cleaning with Freon.

III- TEST PROCEDURES

A. Low-Cycle Fatigue

The closed-loop, servo-controlled low-cycle fatigue machine employed in this study was fitted with a specially constructed containment vessel to allow testing in a protective environment. This cylindrical chamber was fabricated from 2-inch diameter pyrex tubing and was inserted between the holding fixtures. This small-volume enclosure (about 170 cm^3) facilitated system purging and allowed the desired protective gas purity levels to be maintained. Neoprene low-force bellows at the top and bottom connected the chamber to the holding fixtures and permitted the normal longitudinal motion of the specimen during cyclic loading. Side-arms on the pyrex containment vessel provided access for the extensometer arms and a special flexible joint provided an effective seal without influencing the strain measurement. Thermocouple lead-throughs were provided near the lower platen so that the thermocouple leads could be routed from within the enclosure to the temperature control system. Specimen heating was effected by an induction coil wound around the external surface of the cylindrical containment chamber.

All the low-cycle fatigue tests in this program were performed using the specimen configuration shown in Figure 3. Such specimens were held in specially designed threaded adaptors to provide an integral assembly that allowed the adaptor to be heated inductively along with the specimen itself. Large mating surfaces were provided between the specimen and the adaptors to

Figure 3

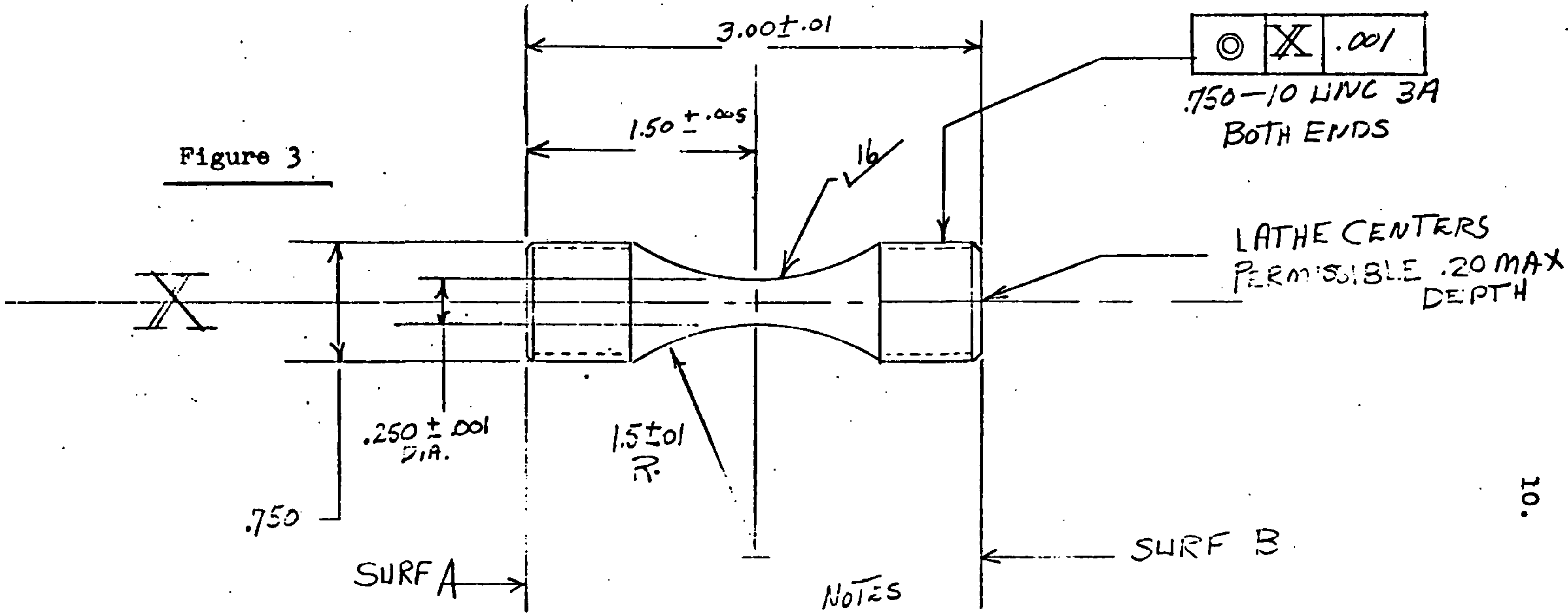

NOTES

1- SURFACES A, & B TO BE PARALLEL WITHIN .001
2- SURFACES A, & B TO BE PERPENDICULAR TO CENTER LINE OF SPECIMEN WITHIN .0005 TIR
3- CONTOURED PORTION OF SPECIMEN TO HAVE A 16 FINISH OR BETTER. FINISHING SHOULD BE IN THE AXIAL DIRECTION USING LOW STRESS LAPPING OR POLISHING OPERATION
4- ~~ALL DIA'S TO BE CONCENTRIC WITHIN .001 TIR~~
5- SCREW THREADS TO BE AS LISTED IN NBS HANDBOOK H 28

UNLESS OTHERWISE SPECIFIED DIMENSIONS ARE IN INCHES
TOLERANCES ON
FRACTIONS ± DECIMALS ± ANGLES ±
ALL SURFACES 32
MATERIAL
GOVT. OR COML. TO BE SPECIFIED

DRAWN
DATE
APPD
ISSUED

APPROVED	DATE
ENGR JTR	1-12-71
MFG	
MATL	

SPECIMEN

LOW CYCLE FATIGUE

SCALE 1/1 WT CALC ACTUAL

Mar-Test inc.
CINCINNATI, OHIO

SIZE MTI-1002

CONT ON SHEET SH NO.

minimize the temperature gradient between them. This approach proved to be quite successful and test temperatures to 538°C (1000°F) were achieved quite readily. It was also shown that a very flat longitudinal temperature profile was obtained.

Test temperatures were measured using chromel-alumel thermocouples spot-welded to the top surface of the bottom adaptor. Special pre-test calibrations performed in a previous study employed thermocouples peened into the surface of a copper specimen and these were used to establish the fact that the temperature of the adaptor which was in direct contact with the copper specimen was within 1°C (2°F) of the specimen temperature measured at the longitudinal midpoint. These tests confirmed the idea that the temperature of a copper specimen, mounted as described above, could be accurately measured and controlled through the use of a thermocouple attached to the adaptor.

Because of the temperature uniformity in the specimen-adaptor assembly a special precaution must be taken to avoid failure in the threaded portion of the specimen. This involves the provision of a large specimen diameter in the grip region compared to the diameter at the specimen midpoint. This was also sufficient to avoid plastic deformation at the specimen-adaptor contact point and therefore to prevent backlash and alignment changes during strain cycling.

A fully instrumented test specimen-adaptor assembly was mounted in the holding fixture of the fatigue machine using a split collet type of assembly and a special leveling device was employed to assure that the specimen was installed perpendicular to the platens. A flat load cell (see previous section) in series with the specimen was used to measure the load applied to the specimen throughout the test.

Once the specimen was installed within the containment vessel the system was purged using a high flow rate of high purity argon (see below for inert gas specifications) for 30 minutes. This established the desired purity level within the test chamber. The inert gas flow rate was then lowered to a few cm^3/min and maintained at this level throughout the test.

Before any tests were initiated the analog strain computer was calibrated by making use of values for Young's modulus (an E value of 6.895×10^4 MN/m^2 for 538°C was used in all copper and copper alloy tests; a value of 4.49×10^4 MN/m^2 at 538°C was used in a subsequent calibration for the tests of pure silver) and specimen cross-sectional area (A). These values were used as shown in the block diagram in Figure 4 to generate axial strain values corresponding to measured values of diametral strain and force. This diagram provides an aid to an understanding of the computer calibration procedure. The values of A and E were used to adjust the compliance control to establish the following equality:

$$AE = F/\epsilon_e \qquad (1)$$

Prior to heating a specimen to the desired test temperature the system was placed in force control. This automatically kept the force at zero by gradually lowering the movable platen

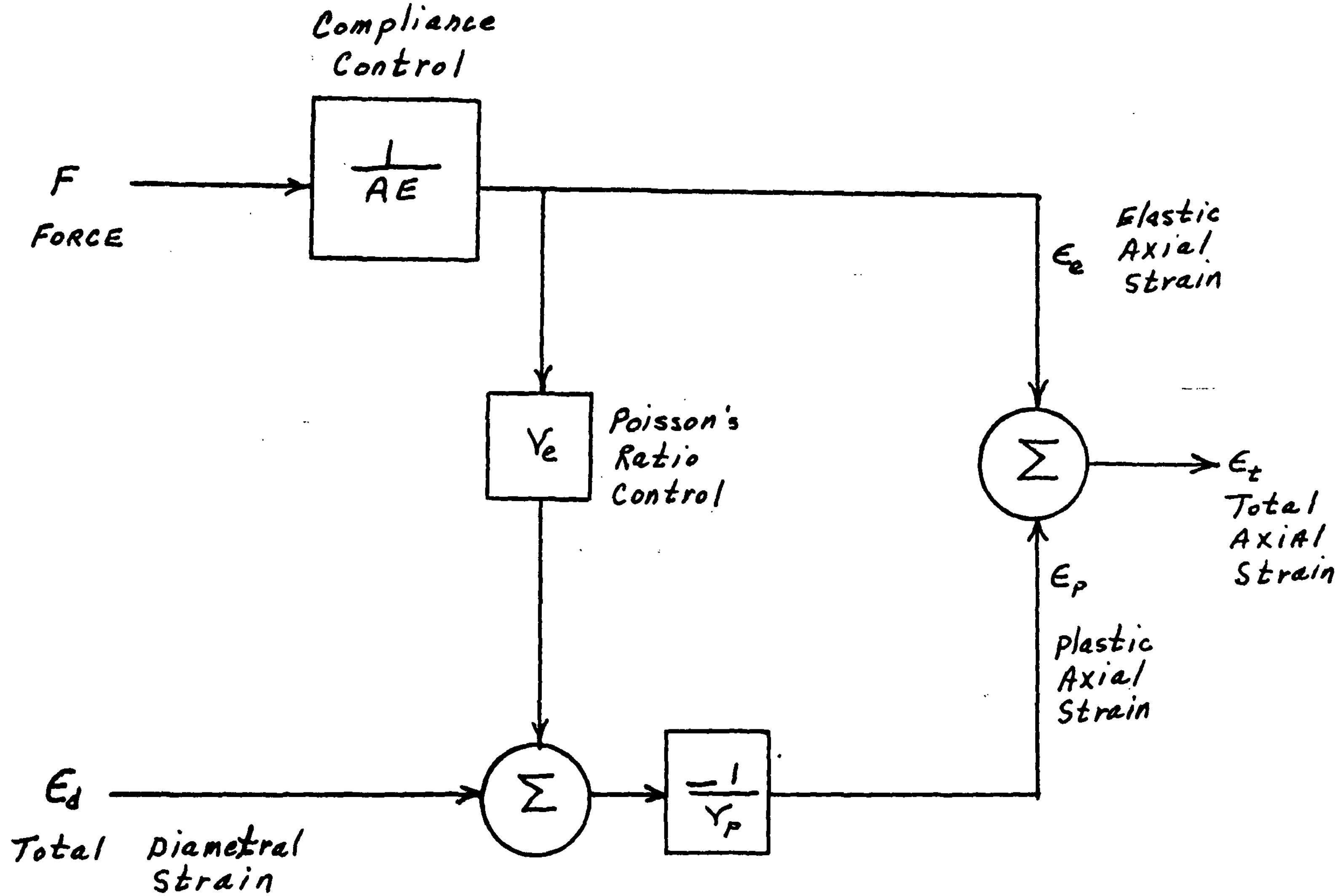

Figure 4- Block Diagram of Strain Computer

to account for the thermal expansion of the specimen as the temperature was increased. When test temperature was obtained the analog strain computer was employed to yield a value for Poisson's ratio. The specimen was cycled elastically so that the actual plastic strain, $\Delta\epsilon_p$, was zero and the value of Poisson's ratio could be obtained by the ratio of the diametral to axial strain; thus:

$$\nu_e = - \frac{\epsilon_d}{\epsilon_e} \qquad (2)$$

The ν_e control on the computer was then adjusted to force the computer value of $\Delta\epsilon_p$ to zero. At this point the above relations were satisfied and the correct value of ν_e was indicated on a potentiometer turns-counting dial on the computer panel (the value for Poisson's ratio plastic was set internally to 0.5 in accordance with constant volume deformation conditions associated with plastic deformation). At this point the computer was calibrated and furnished a correct axial strain signal for recording and control purposes.

With the computer calibration complete the test was ready to begin. Two recorders were connected to the console, one to monitor load and the other to monitor the total axial strain. The system was placed in automatic control and the strain was gradually increased to the desired level. This gradual increase to the desired strain level requires 5 or 6 cycles and avoids specimen damage due to "overshooting" the strain range which can occur if an attempt is made to impose the desired strain level on the first loading cycle. When the desired strain range was reached the test conditions were kept constant until fracture occurred.

Hysteresis loops were recorded on an x-y recorder during the first few cycles and at frequent intervals thereafter. In addition, a continuous recording was made of the applied load and the associated plastic strain. When the specimen fractured, the shut-down circuit automatically de-energized the entire testing system including the induction generator, the hydraulic ram, the timing device and the recorders. However, the protective environment system remained functional until the specimen cooled to room temperature.

High purity (guaranteed 99.999% purity or better) argon gas was employed as the protective environment on this test program. When a slight surface tarnishing was noted in the first few tests it was decided to use the same high purity argon gas but with an additive of 1000 ppm of hydrogen so as to provide a slightly reducing atmosphere. As another protective measure a small (about 6 cm^2 in area) piece of 0.01 cm thick tantalum sheet was spot-welded to the upper specimen adaptor. This getter foil was actually positioned to allow it to protrude about 1/8 inch below the bottom surface of the adaptor so that the induction field would heat this region of the getter to a temperature that was slightly higher than the test temperature. In this way an effective gettering action was achieved to increase the purity level of the test atmosphere. This approach was employed in all tests at 538°C (1000°F); all room temperature tests were performed in air.

B. Short-Term Tensile

Measurements of short-term tensile behavior were made using the same hydraulically-actuated, servo-controlled fatigue machines employed in the low-cycle fatigue evaluations. Furthermore, the same specimen design was employed and the specimen preparation, test environment, installation and instrumentation procedures were identical to those employed in the fatigue tests. These short-term tensile tests were performed using a diametral extensometer and the true diametral strain rate was kept constant at $1x10^{-3}$ sec^{-1} (the corresponding axial strain rate was, therefore, about $2x10^{-3}$ sec^{-1}). In many of these tests the specimen began to "neck down" at a location just above or below the point at which the extensometer was positioned to give a local strain rate higher than the control value. Since necking occurs beyond the ultimate tensile strength point it is felt that the ultimate and yield strengths are not affected by this behavior. It might, however, have an effect on the reduction in area although there was no definite indication that this property was significantly affected. For example, in the R-2-8 test the specimen necked down at or at least very close to the extensometer position. In the R-2-1 test, however, this was not the case and the strain rate at the necked down region was higher than the control value. Both tests yielded the same reduction in area values to indicate that this necking down problem had no significant effect in these evaluations.

IV- TEST DATA

A. Short-Term Tensile

The short-term tensile properties measured at room temperature in air and at 538°C in argon are summarized in

Tables T1 and T2. Duplicate tests were performed for each material at each test temperature and the load versus strain traces were analyzed to yield the reported values for the ultimate and yield strengths. A post-test measurement of the fractured specimen led to the reported values of the reduction in area. All these tests were performed using a true axial strain rate of 2×10^{-3} sec^{-1}.

B. Low-Cycle Fatigue

Summary data* obtained for the 12 materials evaluated in Task 1 are presented in Tables F-0 through F-13. Plots of the total strain range versus cycles to failure are presented in Figures F-0 through F-13. Paired curves were drawn to provide a representation of the fatigue behavior and these curves were used to obtain the strain ranges corresponding to cyclic lives of 300 and 3000 cycles. A summary of this information is provided in Table F-14.

C. General Observations

In general, the specimens after test appeared clean and bright to indicate no serious contamination of the specimens during test. In a few series (R-6 for example) one or two specimens did exhibit a slight surface tarnishing but the fatigue life obtained was in excellent agreement with the other data in the series obtained when the specimens were clean and bright after test. Specimens in series R-9 and R-13 were all definitely tarnished after test to indicate that in the environment specified

*Strain range components at $N_f/2$ were calculated from the stress range at this point and the total axial strain range.

in this program these materials will not remain clean and bright at 538°C for the time periods involved.

In a few tests, particularly those at the higher strain ranges in the R-1 and R-2 series, the number of cycles to failure appeared to be much higher than expected based on the lower strain range results. An analysis of the load traces obtained in these tests indicated that the crack propagation period seemed to be inordinately large and it was this which yielded the long fatigue life. For this reason the data summaries for the R-1 and R-2 series included both the N_f value and another value in parentheses to indicate the fatigue life based on another failure criterion. The load versus time traces were studied and failure was arbitrarily chosen as that point at which the length of the cusp in the compression portion of the load trace was 10 percent of the length of the trace corresponding to the compressive load. A plot of this information seemed to provide a more consistent behavior pattern for fatigue life as a function of the total strain range.

Some plastic instability was noted in certain tests which led to "barrelling" of the specimen in the region close to the minimum diameter point. This effect was noted in the highest strain range tests of the R-0, R-1 and R-2 series. It was most pronounced in the R-8 series where a 3 percent strain range test yielded a specimen at fracture which appeared almost as a notched specimen. These observations seem consistent with the reported discussions of barrelling in cyclic strain exposures of certain materials since the extent of barrelling is largest at the highest strain ranges and in the more ductile materials.

TABLE T1 - Short-Term Tensile Properties Measured in Air at Room Temperature Using a Strain Rate of 0.2% per Second

Diametral Extensometer				Hourglass-Shaped Specimens	
Spec. No.	Material	Material Condition	0.2% Offset Yield Strength, MN/m^2	Ultimate Tensile Strength, MN/m^2	Reduction in Area, %
R-0-22	Zr-Cu	Annealed	47.1	246	88
R-0-23	Zr-Cu	Annealed	45.0	243	88
R-1-5	Zr-Cu	1/4 Hard	301	339	51
R-1-7	Zr-Cu	1/4 Hard	299	343	51
R-2-3	Zr-Cu	1/2 Hard	338	378	82
R-2-9	Zr-Cu	1/2 Hard	334	378	81
R-3-6	Te-Cu	1/2 Hard	356	360	36
R-3-11	Te-Cu	1/2 Hard	353	360	39
R-4-7	Cr-Cu	SA & Aged	518	527	58
R-4-13	Cr-Cu	SA & Aged	523	531	55
R-5-7	OFHC Cu	Hard	305	317	81
R-5-13	OFHC Cu	Hard	312	317	83 (slight oval)
R-6-7	OFHC Cu	1/4 Hard	302	341	66
R-6-13	OFHC Cu	1/4 Hard	312	338	64
R-7-8	OFHC Cu	Annealed	37.3	233	82
R-7-10	OFHC Cu	Annealed	40.0	233	80

TABLE T1 continued

Diametral Extensometer				Hourglass-Shaped Specimens	
Spec. No.	Material	Material Condition	0.2% Offset Yield Strength, MN/m^2	Ultimate Tensile Strength, MN/m^2	Reduction in Area, %
R-8-1	Ag	As Drawn	286	290	86
R-8-6*	Ag	As Drawn	276	291	88
R-8-11	Ag	As Drawn	281	289	85
R-9-6	Zr-Cr-MgCu	SA, CW & Aged	537	551	77
R-9-13	Zr-Cr-MgCu	SA, CW & Aged	536	549	77
R-10-6	Electroformed Cu	30-35 ksi	110	231	48 } oval shaped
R-10-10	Electroformed Cu	30-35 ksi	105	224	57 } oval shaped
R-13-2	Co-Be-Zr-Cu	SA and Aged	347	497	48
R-13-4	Co-Be-Zr Cu	SA and Aged	344	500	48

*Specimen R-8-6 was inadvertently tested in load control; this data point is reported because it represents interesting information since the strain rate was approximately two orders of magnitude higher than that used in the other tests.

TABLE F2 - Short-Term Tensile Properties Measured in Argon at 538°C Using a Strain Rate of 0.2% per Second

Diametral Extensometer				Hourglass-Shaped Specimens	
Spec. No.	Material	Material Condition	0.2% Offset Yield Strength, MN/m^2	Ultimate Tensile Strength, MN/m^2	Reduction in Area, %
R-0-16	Zr-Cu	Annealed	29.6	84.8	95
R-0-18	Zr-Cu	Annealed	36.5	86.8	96
R-1-6	Zr-Cu	1/4 Hard	215	218	84
R-1-2	Zr-Cu	1/4 Hard	178	179.5	87
R-1-8	Zr-Cu	1/4 Hard	191	196	84
R-2-1	Zr-Cu	1/2 Hard	223	226	84
R-2-8	Zr-Cu	1/2 Hard	202	207	84
R-3-3	Te-Cu	1/2 Hard	24.1	71.0	26
R-3-12	Te-Cu	1/2 Hard	25.4	77.3	30
R-4-6	Cr-Cu	SA & Aged	251	261	16
R-4-12	Cr-Cu	SA & Aged	258	263	19
R-5-12	OFHC Cu	Hard	22.1	69.6	66
R-5-6	OFHC Cu	Hard	24.8	71.0	64
R-6-6	OFHC Cu	1/4 Hard	16.6	69.6	26
R-6-12	OFHC Cu	1/4 Hard	16.6	66.2	30 (slight oval)

TABLE T2 continued

Diametral Extensometer				Hourglass-Shaped Specimens	
Spec. No.	Material	Material Condition	0.2% Offset Yield Strength, MN/m^2	Ultimate Tensile Strength, MN/m^2	Reduction in Area, %
R-7-13	OFHC Cu	Annealed	21.4	60.7	54
R-7-11	OFHC Cu	Annealed	25.5	61.4	48
R-8-12	Ag	As Drawn	17.9	34.8	99
R-8-4	Ag	As Drawn	15.9	33.6	99
R-9-5	Zr-Cr-MgCu	SA, CW & Aged	295	311	39
R-9-12	Zr-Cr-MgCu	SA, CW & Aged	296	306	42
R-10-2	Electroformed Cu	30-35 ksi	36.2	46.2	5
R-10-9	Electroformed Cu	30-35 ksi	32.4	44.8	5
R-13-3	Co-Be-Zr Cu	SA and Aged	241	259	8
R-13-9	Co-Be-Zr Cu	SA and Aged	245	262	8

TABLE F-0 - LOW-CYCLE FATIGUE TEST RESULTS OBTAINED IN ARGON AT 538°C USING A STRAIN RATE OF $2x10^{-3}$ SEC^{-1}.

R-0 Series
Zirconium Copper; annealed

Axial Strain Control
A-ratio of infinity
$E = 6.895 \times 10^4$ MN/m^2

Spec. No.	Poisson's Ratio	Total Strain Range, %	Stress Range at Start, MN/m^2	at $N_f/2$ $\Delta\epsilon_p$ %	at $N_f/2$ $\Delta\epsilon_e$ %	at $N_f/2$ $\Delta\sigma$ MN/m^2	N_f, Cycles to Failure	Remarks
R-0-14	0.29	2.0	120	1.82	0.18	124	1,512	Hardened then Softened
R-0-15	0.29	1.5	100	1.35	0.15	103.5	4,188	Hardened then Softened
R-0-25	0.295	3.5	131	3.29	0.21	145	283	Hardened
R-0-17	0.29	3.0	119.5	2.79	0.21	142	307	Hardened
R-0-19	0.29	1.7	119.5	1.52	0.18	124	2,300	Hardened then Softened
R-0-21	0.29	2.5	119.5	2.30	0.20	138	418	Hardened

TABLE F-1 - LOW-CYCLE FATIGUE TEST RESULTS OBTAINED IN ARGON AT 538°C USING A STRAIN RATE OF 2×10^{-3} SEC^{-1}.

R - 1 Series
Zirconium Copper; 1/4 Hard

Axial Strain Control
A - ratio of infinity
$E = 6.895 \times 10^{4}$ MN/m^2

Spec. No.	Poisson's Ratio	Total Strain Range, %	Stress Range at Start, MN/m^2	at $N_f/2$: $\Delta\epsilon_p$ %	at $N_f/2$: $\Delta\epsilon_e$ %	at $N_f/2$: $\Delta\sigma$ MN/m^2	N_f^*, Cycles to Failure	Remarks
R-1-3	0.33	2.5	362	2.21	0.29	197.5	524 (385)	Softened
R-1-4	0.32	1.6	365	$\cancel{1.27}$	0.33	225	1,088 (975)	Softened
R-1-9	0.33	3.5	352	3.3	0.20	137	562 (198)	Softened
R-1-10	0.32	3.5	359	3.24	0.26	179.5	447 (235)	Softened
R-1-11	0.32	1.2	369	0.99	0.21	143	5590 (5200)	Softened
R-1-12	0.32	1.35	370	1.11	0.24	167	3,660 (3400)	Softened

*Numbers in parentheses represent an alternate failure criterion as discussed on page 18 of text.

TABLE F-2 - LOW-CYCLE FATIGUE TEST RESULTS OBTAINED IN ARGON AT 538°C USING A STRAIN RATE OF 2×10^{-3} SEC^{-1}.

R- 2 Series
Zirconium Copper; 1/2 Hard

Axial Strain Control
A - ratio of infinity
$E = 6.895 \times 10^{4}$ MN/m^2

Spec. No.	Poisson's Ratio	Total Strain Range, %	Stress Range at Start, MN/m^2	at $N_f/2$ $\Delta\epsilon_p$ %	$\Delta\epsilon_e$ %	$\Delta\sigma$ MN/m^2	N_f^*, Cycles to Failure	Remarks
R-2-2	0.30	3.0	372	2.826	0.174	120	1615 (1140)	Softened
R-2-4	0.30	5.0	372	4.8	0.2	134.5	366 (216)	Softened
R-2-5	0.30	4.0	379	3.81	0.19	131	552 (390)	Softened
R-2-10	0.30	2.8	392	2.62	0.18	124	1,055 (880)	Softened
R-2-11	0.30	2.0	409	1.82	0.18	124	1,239 (720)	Softened
R-2-6	0.285	2.0	407	1.83	0.17	118.5	2,051 (1560)	Softened
R-2-12	0.30	1.7	403	1.51	0.19	130.5	1770 (none)	Softened
R-2-13	0.30	1.5	427	1.30	0.20	134.5	2453 (None)	Softened

TABLE F-3 - LOW-CYCLE FATIGUE TEST RESULTS OBTAINED IN ARGON AT 538°C USING A STRAIN RATE OF 2×10^{-3} SEC^{-1}.

R-3 Series
Tellurium Copper; 1/2 Hard

Axial Strain Control
A - ratio of infinity
$E = 6.895 \times 10^{4}$ MN/m^2

Spec. No.	Poisson's Ratio	Total Strain Range, %	Stress Range at Start, MN/m^2	at $N_f/2$ $\Delta\epsilon_p$ %	$\Delta\epsilon_e$ %	$\Delta\sigma$ MN/m^2	N_f, Cycles to Failure	Remarks
R-3-10	0.33	1.6	80	1.44	0.16	111	390	Hardened
R-3-13	0.33	2.0	73.8	1.84	0.16	109	117	Hardened
R-3-1	0.31	1.2	73.1	1.05	0.15	103.5	462	Hardened
R-3-2	0.31	0.8	67.6	0.65	0.15	103.5	1,179	Hardened
R-3-4	0.31	1.0	71	0.85	0.15	101.5	802	Hardened
R-3-5	0.31	0.5	56.6	0.37	0.13	89	3,908	Hardened

TABLE F-4 - LOW-CYCLE FATIGUE TEST RESULTS OBTAINED IN ARGON AT 538°C USING A STRAIN RATE OF $2x10^{-3}$ SEC^{-1}.

R-4 Series
Chromium Copper; SA and Aged

Axial Strain Control
A - ratio of infinity
$E = 6.895 \times 10^4$ MN/m²

Spec. No.	Poisson's Ratio	Total Strain Range, %	Stress Range at Start, MN/m²	at $N_f/2$ $\Delta\epsilon_p$ %	$\Delta\epsilon_e$ %	$\Delta\sigma$ MN/m²	N_f, Cycles to Failure	Remarks
R-4-1	0.26	2.0	444.0	1.49	0.51	351.0	147	Softened
R-4-2	0.26	1.6	489.0	1.14	0.46	317.0	354	Softened
R-4-3	0.26	1.4	503.0	0.95	0.45	310.0	605	Softened
R-4-4	0.26	1.0	469.0	0.63	0.37	253.0	1,823	Softened
R-4-5	0.26	1.2	489.0	0.80	0.40	277.0	1,102	Softened
R-4-8	0.26	0.9	474.0	0.57	0.33	228.0	3,648	Softened

TABLE F-5 - LOW-CYCLE FATIGUE TEST RESULTS OBTAINED IN ARGON AT 538°C USING A STRAIN RATE OF 2×10^{-3} SEC^{-1}.

R-5 Series
OFHC Copper; Hard

Axial Strain Control
A - ratio of infinity
$E = 6.895 \times 10^4$ MN/m^2

Spec. No.	Poisson's Ratio	Total Strain Range, %	Stress Range at Start, MN/m^2	at $N_f/2$: $\Delta\epsilon_p$ %	at $N_f/2$: $\Delta\epsilon_e$ %	at $N_f/2$: $\Delta\sigma$ MN/m^2	N_f, Cycles to Failure	Remarks
R-5-2	0.33	1.6	74.4	1.46	0.14	95.2	292	Hardened then softened
R-5-11	0.33	2.0	75.8	1.86	0.14	96.5	195	Hardened then softened
R-5-1	0.33	1.0	62.0	0.88	0.12	84.1	679	Hardened then softened
R-5-4	0.33	0.8	57.2	0.68	0.12	79.3	1,295	Hardened then softened
R-5-3	0.33	1.2	67.5	1.07	0.13	87.8	453	Hardened then softened
5-5-5	0.33	0.6	49.6	0.49	0.11	77.3	3,606	Hardened then softened

TABLE F-6 - LOW-CYCLE FATIGUE TEST RESULTS OBTAINED IN ARGON AT 538°C USING A STRAIN RATE OF $2x10^{-3}$ SEC^{-1}.

R-6 Series
OFHC Copper; 1/4 Hard

Axial Strain Control
A- ratio of infinity
$E = 6.895 \times 10^4$ MN/m^2

				at $N_f/2$			N_f,	
Spec. No.	Poisson's Ratio	Total Strain Range, %	Stress Range at Start, MN/m^2	$\Delta\epsilon_p$ %	$\Delta\epsilon_e$ %	$\Delta\sigma$ MN/m^2	Cycles to Failure	Remarks
R-6-1	0.33	1.6	62.1	1.46	0.14	97.4	85	Hardened
R-6-3	0.32	0.6	37.9	0.49	0.11	77.3	691	Hardened
R-6-4	0.32	0.7	42.8	0.58	0.12	80.7	418	Hardened
R-6-5	0.32	2.0	64.8	1.844	0.156	107.5	56	Hardened
R-6-8	0.32	0.5	42.8	0.39	0.11	75.2	1358	Hardened
R-6-9	0.32	1.0	48.3	0.875	0.125	86.2	200	Hardened
R-6-11	0.32	1.0	49.6	0.876	0.124	85.5	303	Hardened

TABLE F-7 - LOW-CYCLE FATIGUE TEST RESULTS OBTAINED IN ARGON AT 538°C USING A STRAIN RATE OF $2x10^{-3}$ SEC^{-1}.

R-7 Series
OFHC Copper; annealed

Axial Strain Control
A - ratio of infinity
$E = 6.895 \times 10^{4}$ MN/m^2

Spec. No.	Poisson's Ratio	Total Strain Range, %	Stress Range at Start, MN/m^2	at $N_f/2$			N_f, Cycles to Failure	Remarks
				$\Delta\epsilon_p$ %	$\Delta\epsilon_e$ %	$\Delta\sigma$ MN/m^2		
R-7-3	0.33	2.0	78.6	1.86	0.14	93.8	126	Hardened then softened
R-7-4	0.33	1.5	77.2	1.37	0.13	87.5	269	Hardened then softened
R-7-1	0.33	1.2	62.0	1.07	0.13	87.5	437	Hardened then softened
R-7-2	0.33	1.0	68.9	0.88	0.12	83.1	710	Hardened then softened
R-7-7	0.33	0.8	62.0	0.68	0.12	80.7	1313	Hardened then softened
R-7-9	0.34	0.7	55.2	0.58	0.12	81.3	1613	Hardened then softened

TABLE F-8 - LOW-CYCLE FATIGUE TEST RESULTS OBTAINED IN ARGON AT 538°C USING A STRAIN RATE OF $2x10^{-3}$ SEC^{-1}.

R-8 Series
Silver; As drawn

Axial Strain Control
A-ratio of infinity
$E = 4.49 \times 10^4$ MN/m^2

Spec. No.	Poisson's Ratio	Total Strain Range, %	Stress Range at Start, MN/m^2	at $N_f/2$ $\Delta\epsilon_p$ %	$\Delta\epsilon_e$ %	$\Delta\sigma$ MN/m^2	N_f, Cycles to Failure	Remarks
R-8-7	0.37	3.0	58	2.83	0.17	75.9	344	Hardened
R-8-5	0.36	2.5	53.8	2.33	0.17	77.3	603	Hardened
R-8-9	0.36	1.2	42.8	1.07	0.13	57.3	1,902	Hardened
R-8-3	0.36	1.0	40.7	0.875	0.125	55.9	2,620	Hardened
R-8-2	0.36	2.0-	50.4	1.85	0.15	69.0	928	Hardened
R-8-10	0.36	1.5	52.4	1.35	0.15	65.5	1,381	Hardened

NOTE: All specimens barrelled rather severely.

TABLE F-9 - LOW-CYCLE FATIGUE TEST RESULTS OBTAINED IN ARGON AT 538°C USING A STRAIN RATE OF $2x10^{-3}$ SEC^{-1}.

R-9 Series
Zr-Cr-Mg Copper; SA, CW and Aged

Axial Strain Control
A - ratio of infinity
$E = 6.895 \times 10^4$ MN/m^2

Spec. No.	Poisson's Ratio	Total Strain Range, %	Stress Range at Start, MN/m^2	at $N_f/2$ $\Delta\epsilon_p$ %	at $N_f/2$ $\Delta\epsilon_e$ %	at $N_f/2$ $\Delta\sigma$ MN/m^2	N_f, Cycles to Failure	Remarks
R-9-11	0.31	2.0	555	1.46	0.54	374	843	Softened
R-9-4	0.31	3.0	555	2.42	0.58	397	357	Softened
R-9-1	0.30	2.25	566	1.68	0.57	393	500	Softened
R-9-3	0.30	2.5	585	1.87	0.63	435	346	Softened
R-9-8	0.30	1.4	574	0.86	0.54	373	2000	Softened
R-9-2	0.295	1.2	545	0.64	0.56	388	1,317	Softened
R-9-9	0.30	0.9	510	0.41	0.49	338	6,670	Softened

TABLE F-10 - LOW-CYCLE FATIGUE TEST RESULTS OBTAINED IN ARGON AT 538°C USING A STRAIN RATE OF 2×10^{-3} SEC^{-1}.

R-10 Series
Electroformed Copper; 30-35 ksi

Axial Strain Control
A - ratio of infinity
$E = 6.895 \times 10^{4}$ MN/m^2

Spec. No.	Poisson's Ratio	Total Strain Range, %	Stress Range at Start, MN/m^2	at $N_f/2$* $\Delta\epsilon_p$ %	$\Delta\epsilon_e$ %	$\Delta\sigma$ MN/m^2	N_f, Cycles to Failure	Remarks
R-10-3	0.37	2.0	92.5	1.9	0.1	69.0	148	Hardened then softened
R-10-4	0.32	1.6	104	1.44	0.16	110	38	Hardened then softened
R-10-1	0.32	0.8	84.1	0.715	0.085	58.6	1,542	Hardened then softened
R-10-8	0.31	1.2	117	1.06	0.14	96.5	72	Hardened then softened
R-10-5	0.32	1.0	92.5	0.895	0.105	72.4	512	Hardened then softened
R-10-7	0.34	0.75	75.7	0.65	0.10	65.5	1,866	Hardened then softened

*Since this material was found to be anisotropic the values for total and plastic strain range are not reliable.

TABLE F-13 - LOW-CYCLE FATIGUE TEST RESULTS OBTAINED IN ARGON AT 538°C USING A STRAIN RATE OF $2x10^{-3}$ SEC^{-1}.

R-13 Series
Co-Be-Zr Copper; SA and Aged

Axial Strain Control
A - ratio of infinity
E = 6.895×10^{4} MN/m^2

Spec. No.	Poisson's Ratio	Total Strain Range, %	Stress Range at Start, MN/m^2	at $N_f/2$ $\Delta\epsilon_p$ %	$\Delta\epsilon_e$ %	$\Delta\sigma$ MN/m^2	N_f, Cycles to Failure	Remarks
R-13-5	0.248	2.0	531	1.27	0.73	503	90	Softened Slightly
R-13-13	0.25	1.2	497	0.56	0.64	442	644	Softened Slightly
R-13-7	0.246	1.5	503	0.82	0.68	469	212	Softened Slightly
R-13-10	0.248	1.0	497	0.34	0.66	455	680	Softened Slightly
R-13-6	0.23	0.8	442	0.20	0.60	414	1615	Softened Slightly
R-13-8	0.24	0.70	407	0.13	0.57	390	3623	Softened Slightly

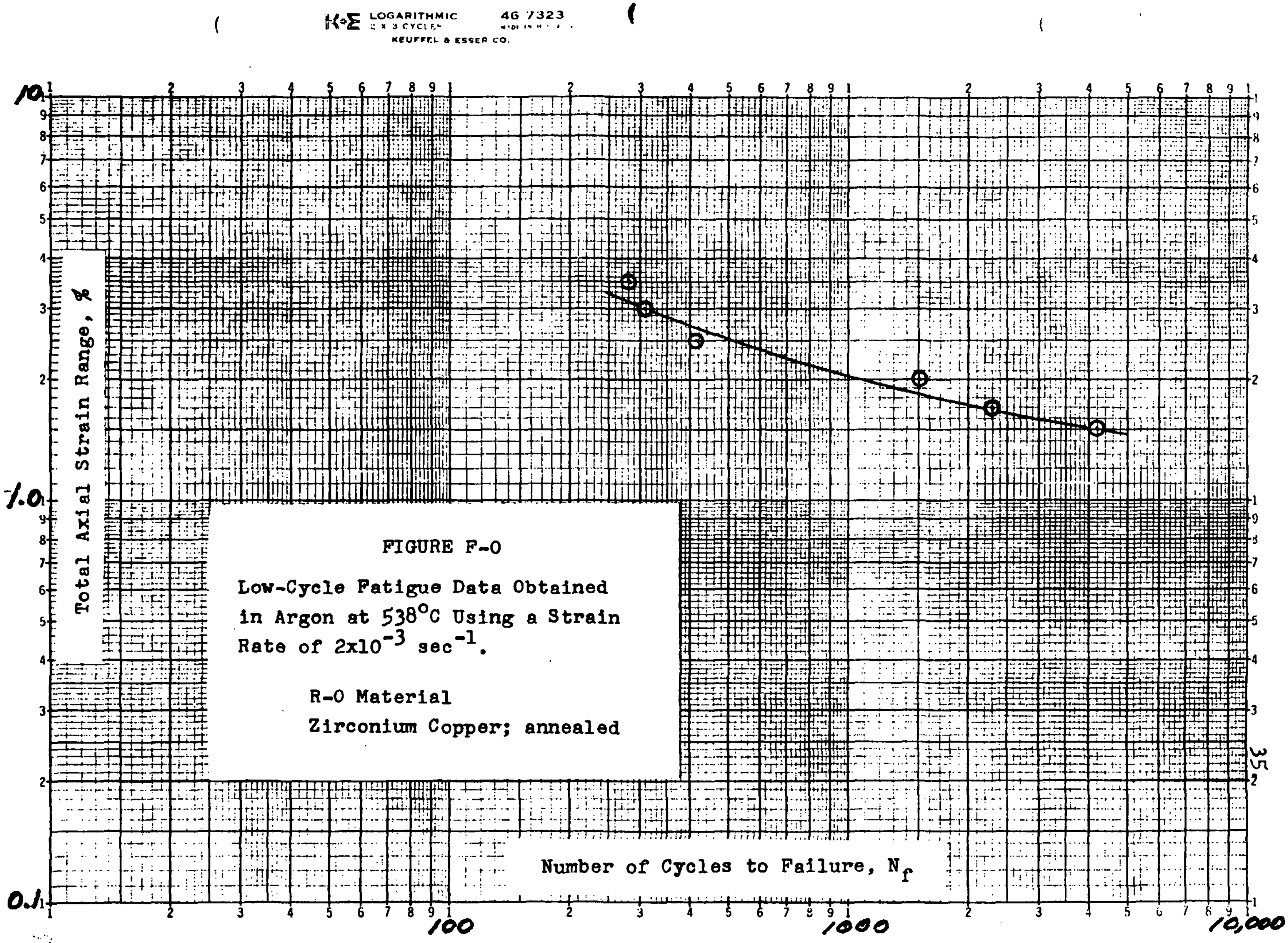

FIGURE F-0

Low-Cycle Fatigue Data Obtained in Argon at 538°C Using a Strain Rate of $2x10^{-3}$ sec^{-1}.

R-0 Material
Zirconium Copper; annealed

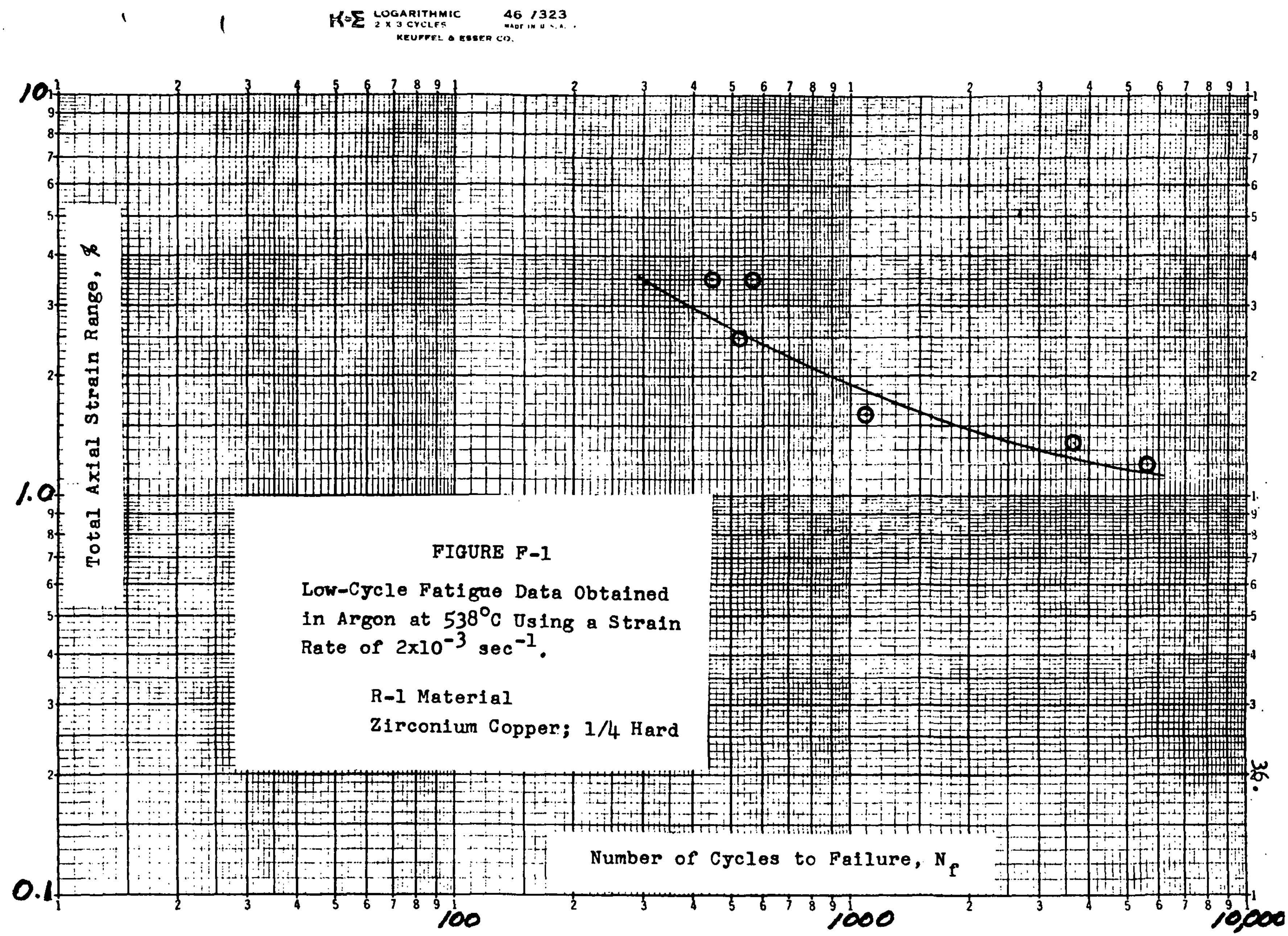

FIGURE F-1

Low-Cycle Fatigue Data Obtained in Argon at 538°C Using a Strain Rate of $2x10^{-3}$ sec^{-1}.

R-1 Material

Zirconium Copper; 1/4 Hard

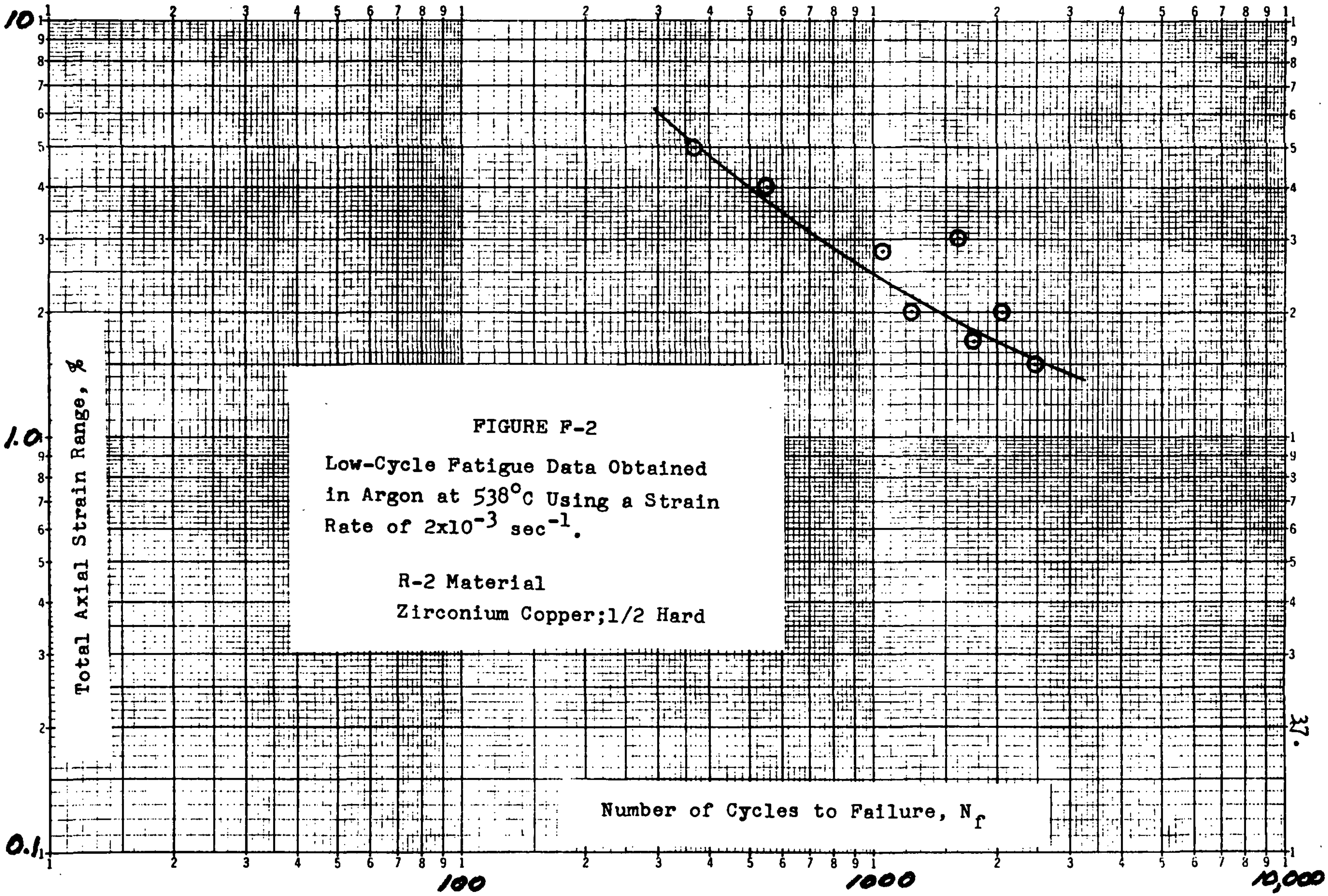

FIGURE F-2

Low-Cycle Fatigue Data Obtained in Argon at 538°C Using a Strain Rate of 2×10^{-3} sec^{-1}.

R-2 Material

Zirconium Copper;1/2 Hard

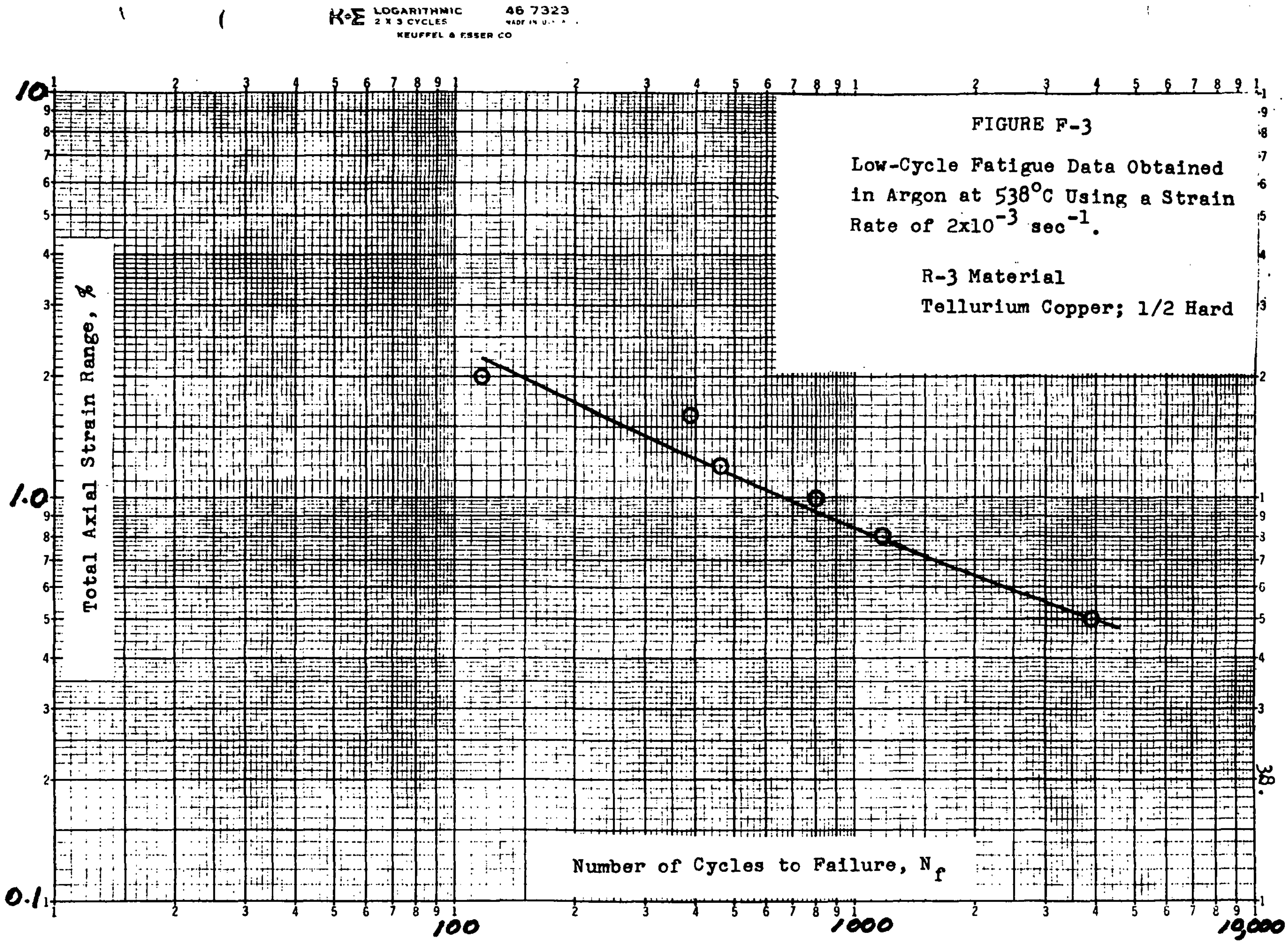

FIGURE F-3

Low-Cycle Fatigue Data Obtained in Argon at 538°C Using a Strain Rate of 2×10^{-3} sec^{-1}.

R-3 Material

Tellurium Copper; 1/2 Hard

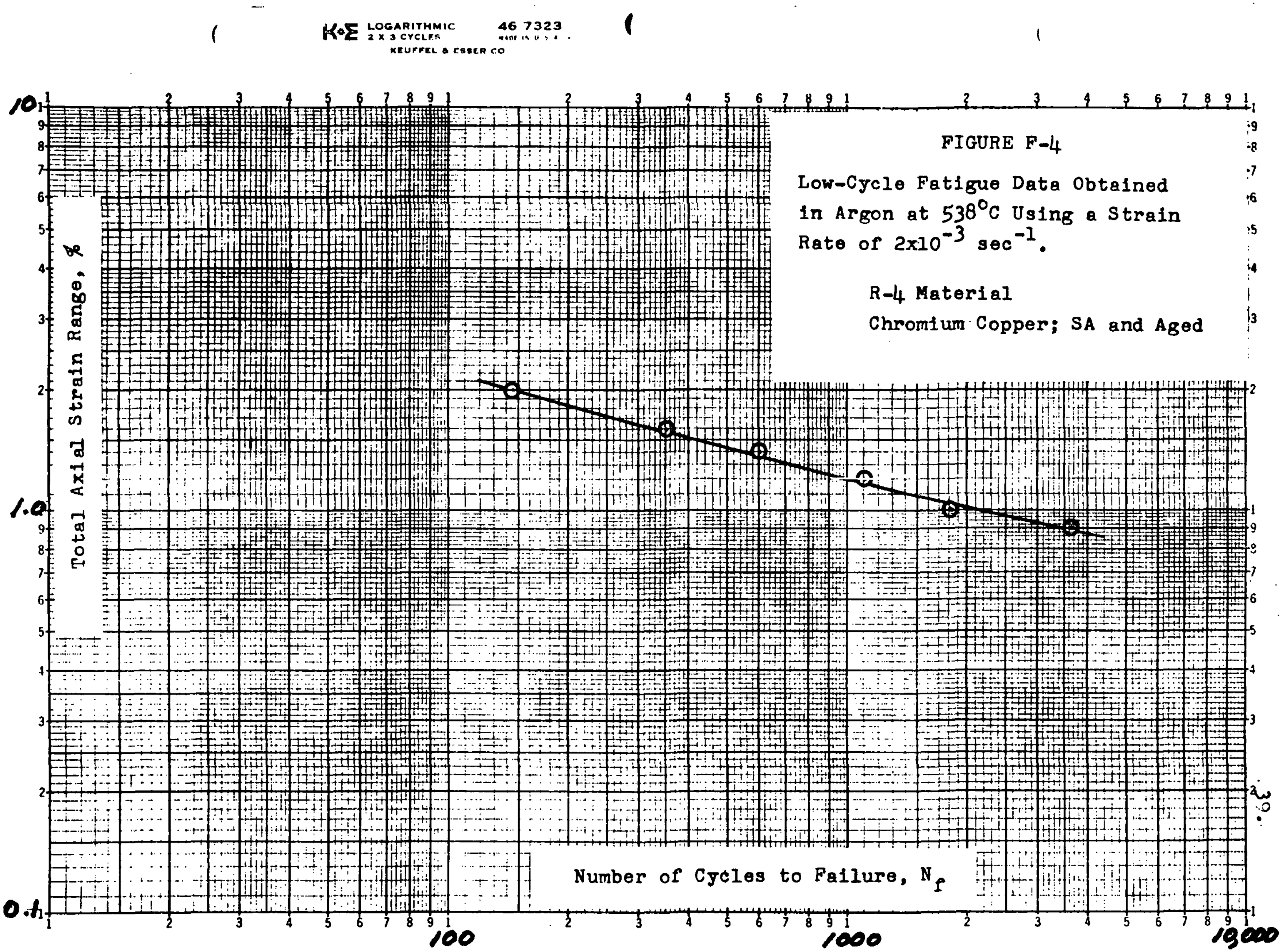
K+E LOGARITHMIC 2 X 3 CYCLES KEUFFEL & ESSER CO 46 7323
FIGURE F-4
Low-Cycle Fatigue Data Obtained in Argon at 538°C Using a Strain Rate of 2x10-3 sec-1.
R-4 Material
Chromium Copper; SA and Aged
Total Axial Strain Range, %
Number of Cycles to Failure, Nf
10
1.0
0.1
100
1000
10,000
30

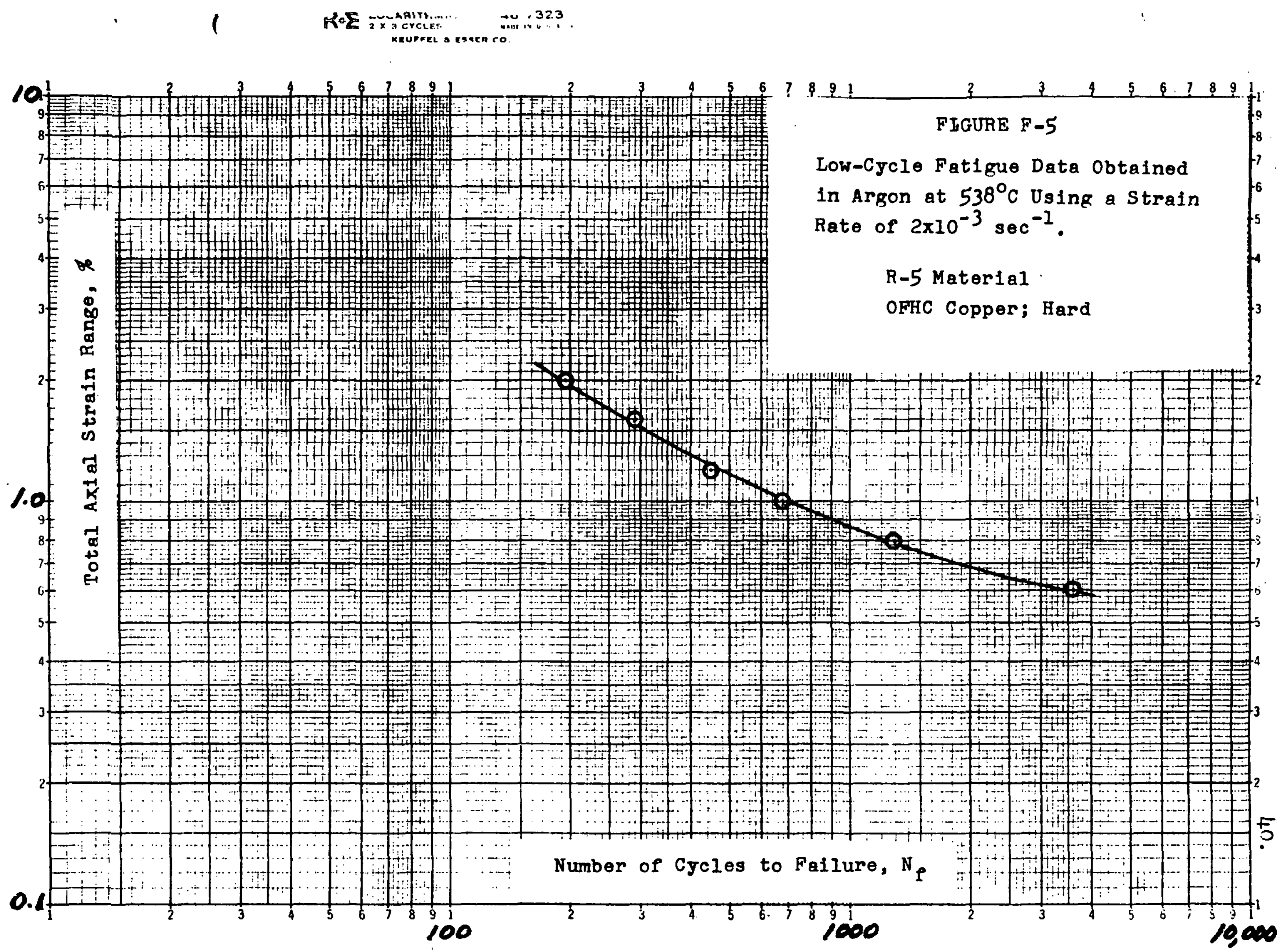
FIGURE F-5
Low-Cycle Fatigue Data Obtained in Argon at 538°C Using a Strain Rate of 2x10-3 sec-1.
R-5 Material
OFHC Copper; Hard
Total Axial Strain Range, %
Number of Cycles to Failure, Nf
10
1.0
0.1
100
1000
10,000

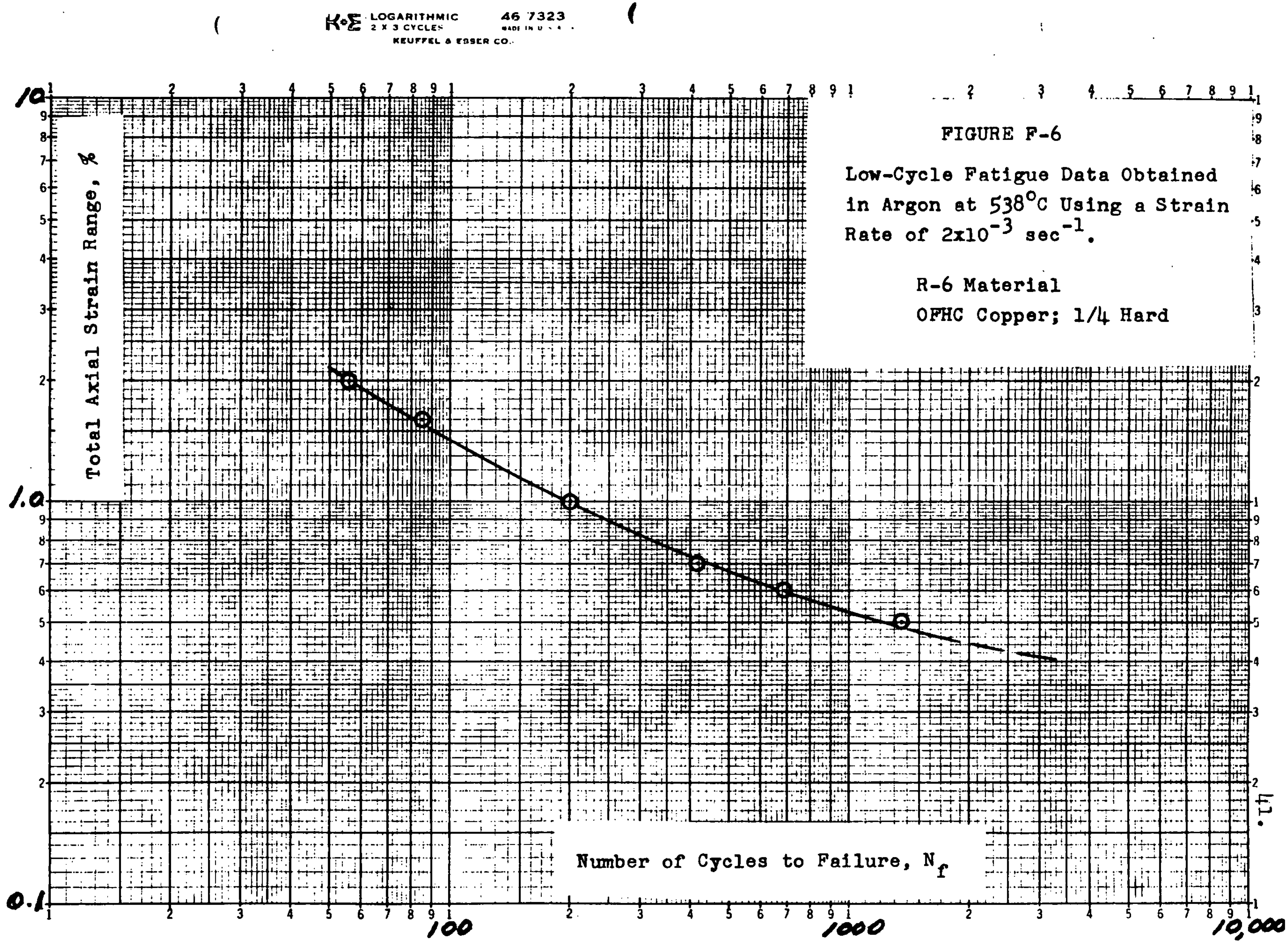

FIGURE F-6

Low-Cycle Fatigue Data Obtained in Argon at 538°C Using a Strain Rate of 2×10^{-3} sec^{-1}.

R-6 Material
OFHC Copper; 1/4 Hard

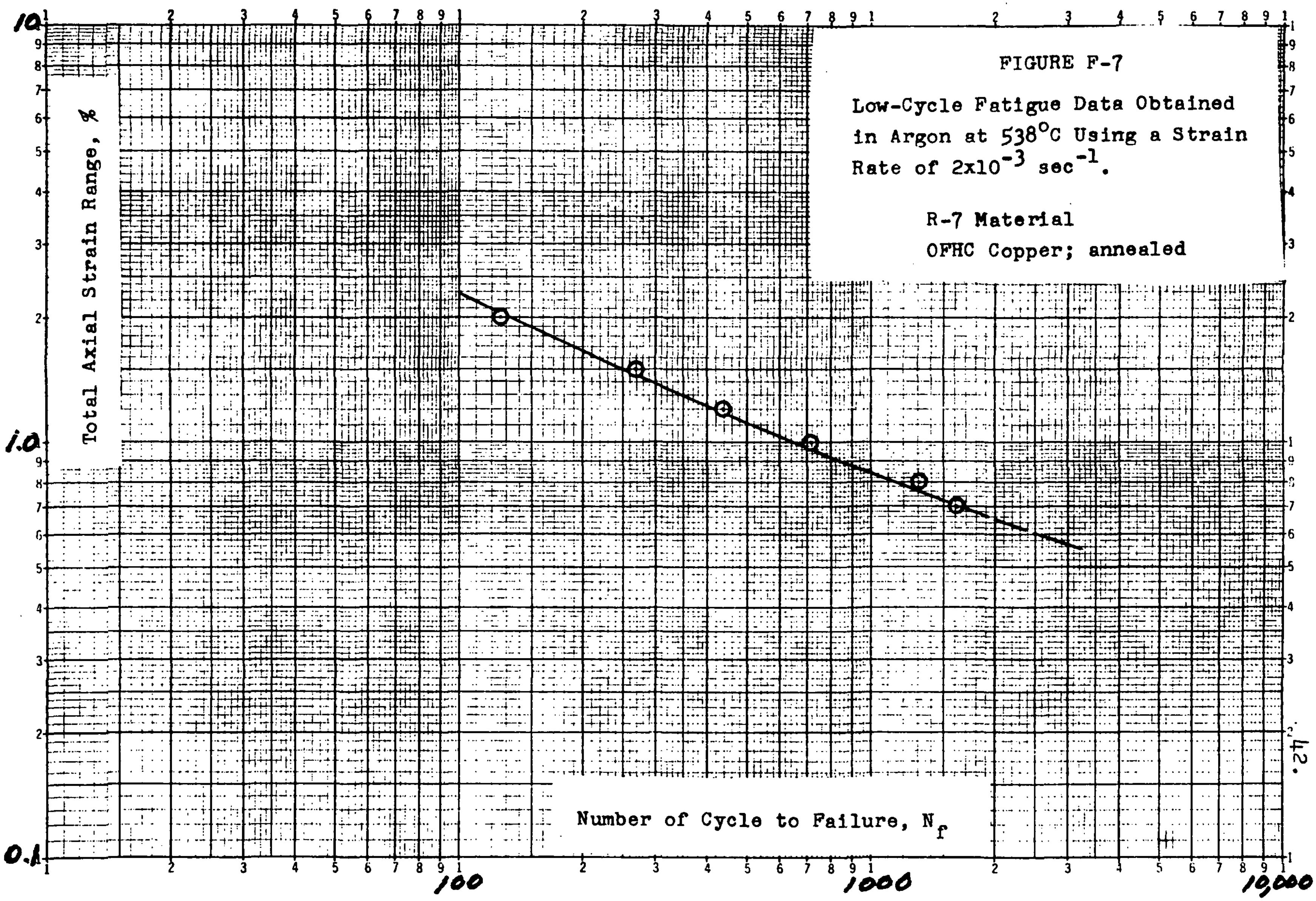
K+E LOGARITHMIC 3 X 3 CYCLES
46 7323
KEUFFEL & ESSER CO.
FIGURE F-7
Low-Cycle Fatigue Data Obtained in Argon at 538°C Using a Strain Rate of 2x10⁻³ sec⁻¹.
R-7 Material
OFHC Copper; annealed
Total Axial Strain Range, %
Number of Cycle to Failure, N_f
10
1.0
0.1
100
1000
10,000

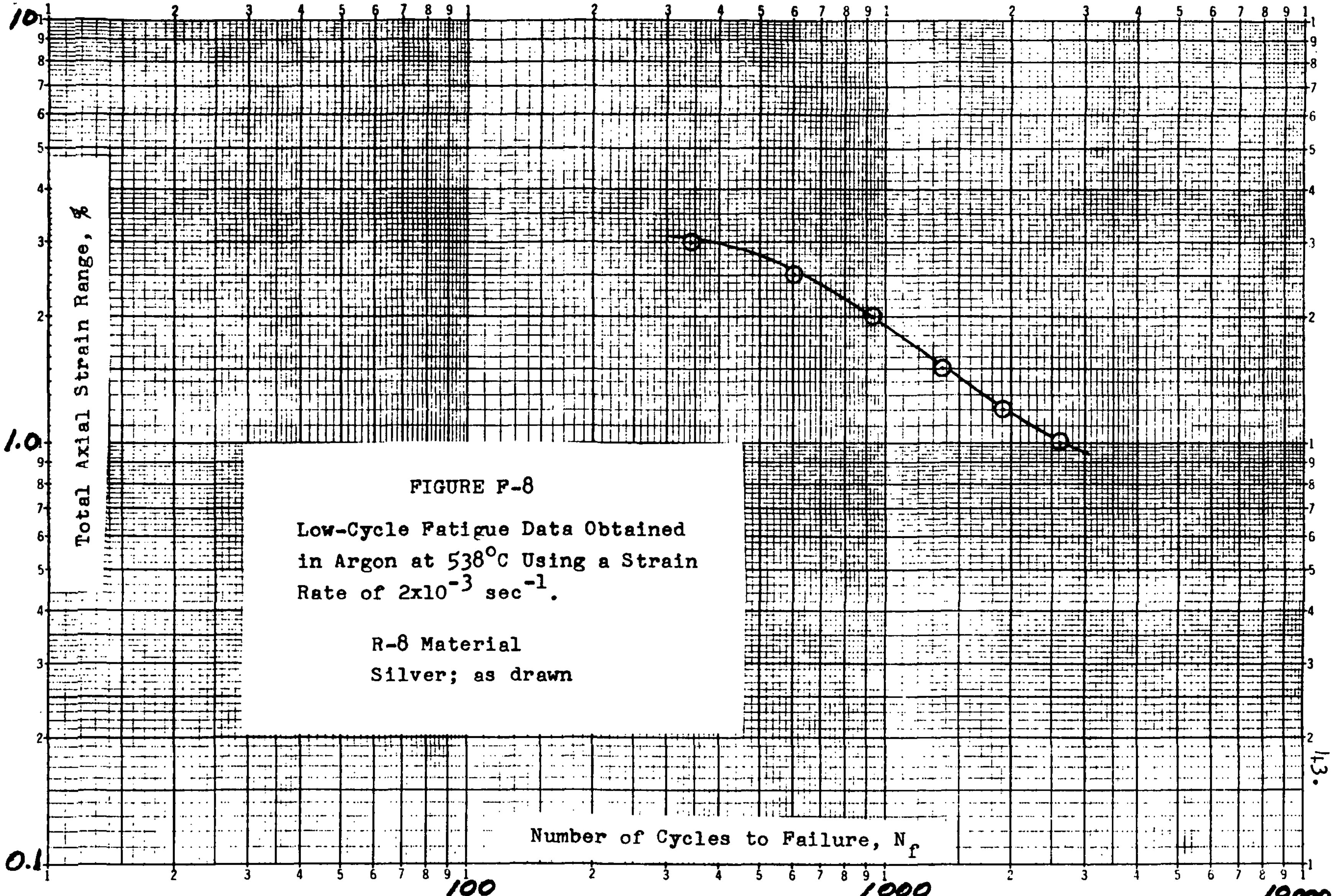

FIGURE F-8

Low-Cycle Fatigue Data Obtained in Argon at 538°C Using a Strain Rate of $2x10^{-3}$ sec^{-1}.

R-8 Material
Silver; as drawn

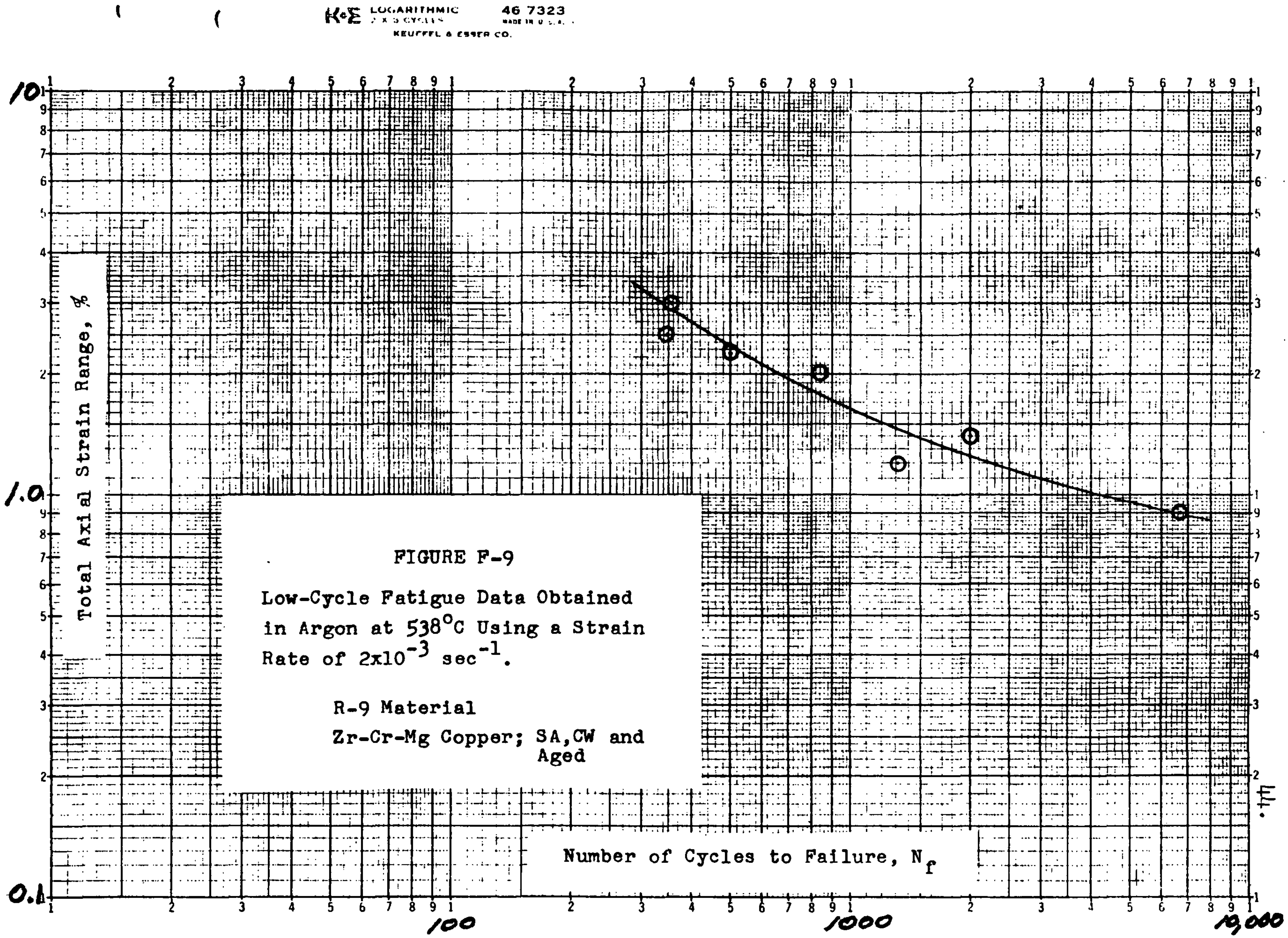

FIGURE F-9

Low-Cycle Fatigue Data Obtained in Argon at 538°C Using a Strain Rate of $2x10^{-3}$ sec^{-1}.

R-9 Material

Zr-Cr-Mg Copper; SA, CW and Aged

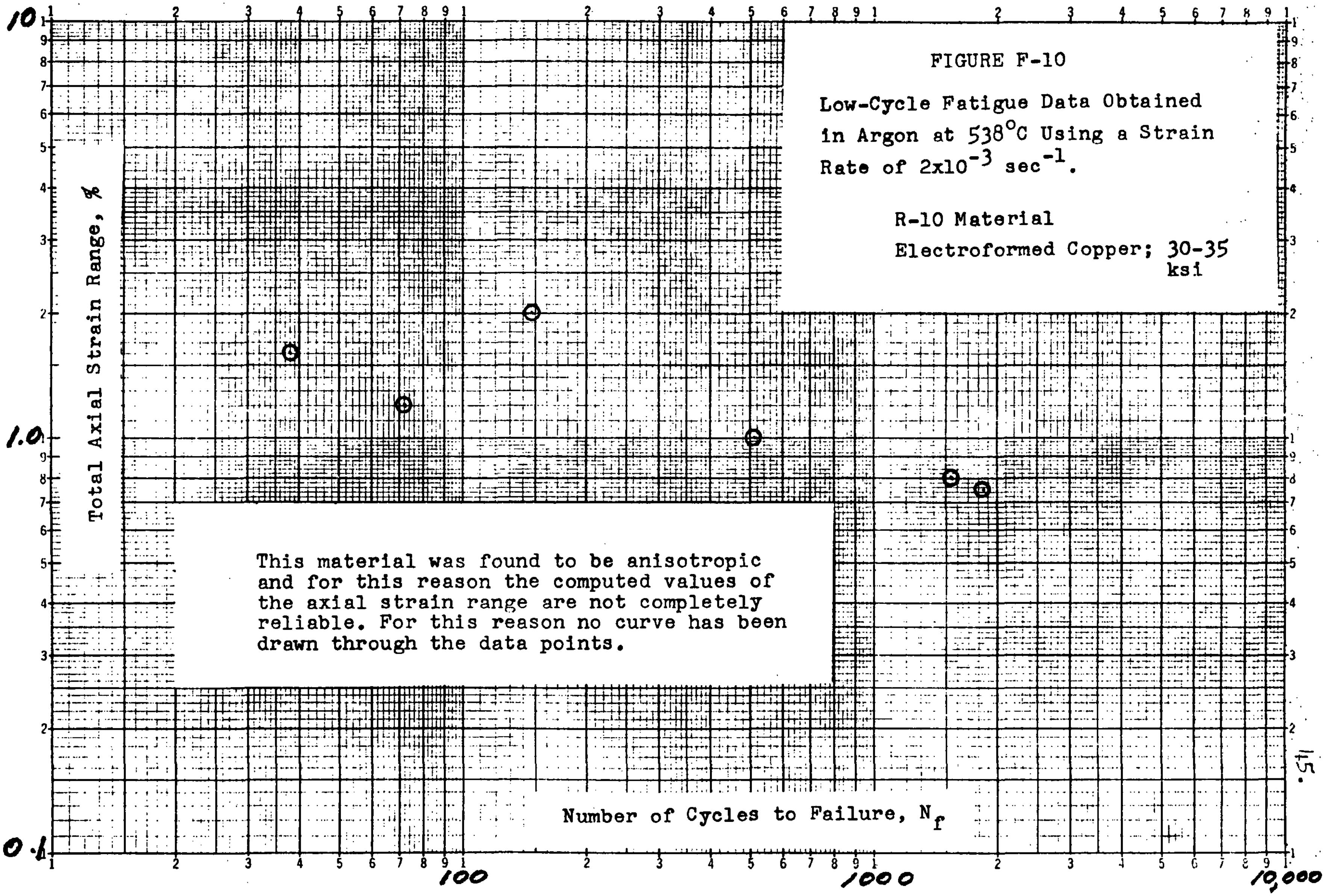

FIGURE F-10

Low-Cycle Fatigue Data Obtained in Argon at 538°C Using a Strain Rate of $2x10^{-3}$ sec^{-1}.

R-10 Material
Electroformed Copper; 30-35 ksi

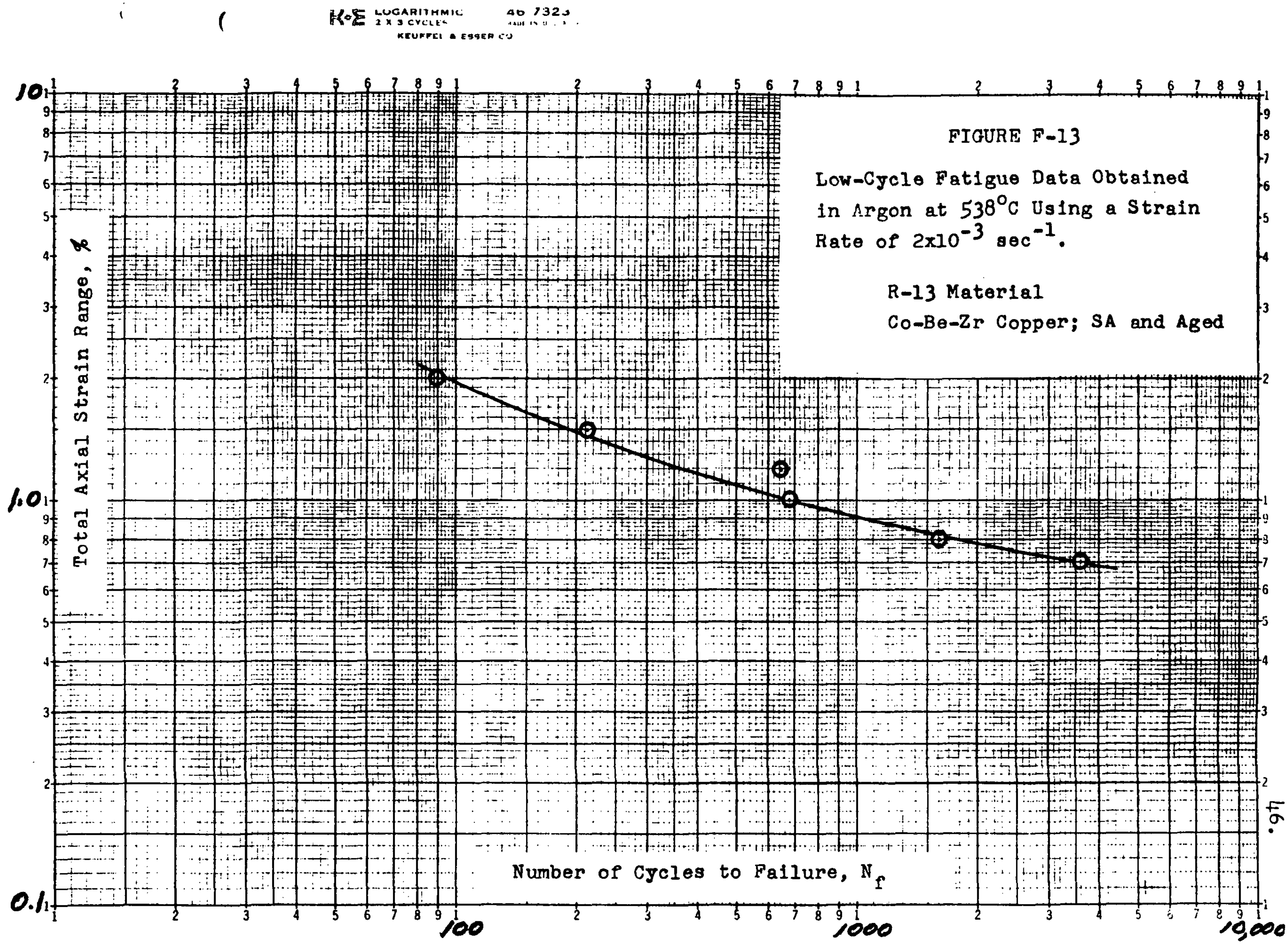
K+E LOGARITHMIC 2 X 3 CYCLES KEUFFEL & ESSER CO. 46 7323
FIGURE F-13
Low-Cycle Fatigue Data Obtained in Argon at 538°C Using a Strain Rate of 2x10-3 sec-1.
R-13 Material
Co-Be-Zr Copper; SA and Aged
Total Axial Strain Range, %
Number of Cycles to Failure, Nf
10
1.0
0.1
100
1000
10,000

TABLE F-14 - Summary of Strain Range Data Obtained in Low-Cycle Fatigue Tests in Argon at 538°C Using a Strain Rate of 2×10^{-3} sec^{-1}.

Series	Material	Material Condition	Total Strain Range, $\Delta\epsilon_t$, in Percent, for Cyclic Life of: 300 cycles	3000 cycles
R-0	Zirconium-Copper	Annealed	3.05	1.6
R-1	Zirconium-Copper	1/4 Hard	3.5	1.3
R-2	Zirconium-Copper	1/2 Hard	6.1	1.41
R-3	Tellurium-Copper	1/2 Hard	1.42	0.55
R-4	Chromium-Copper	SA and Aged	1.64	0.93
R-5	OFHC Copper	Hard	1.52	0.62
R-6	OFHC Copper	1/4 Hard	0.83	0.41
R-7	OFHC Copper	Annealed	1.39	0.57
R-8	Silver	As Drawn	3.1	0.95
R-9	Zr-Cr-Mg Copper	SA, CW and Aged	3.25	1.1
R-10	Electroformed Copper	30-35 ksi	See footnote	
R-13	Co-Be-Zr Copper	SA and Aged	1.29	0.72

The R-10 material was found to be anisotropic and for this reason the computed values of the axial strain range are not completely reliable. In view of this no faired curve was drawn through the data points in Figure F-10 and as a result no values for the 300 and 3000 cycle strain ranges are reported.